DRAFT 25 May 2005

The HST Treasury Program on Eta Carinae

Technical memo number 6 -- May 2005

A MODEL OF THE DISTRIBUTION SCATTERED/DIFFUSE LIGHT ON THE STIS CCD IN SPECTROSCOPIC MODE

John C. Martin, University of Minnesota

(If you use information or advice from this memo, please acknowledge it and the net site http://etacar.umn.edu in any resulting publications; thanks.)

1. Introduction

This report outlines the work done by the Eta Carinae HST Treasury Project to determine the properties and distribution of scattered/diffuse background light on the STIS CCD in spectroscopic mode. In this document we present a model for the scattered/diffuse background light as a function of wavelength. We wish to emphasize that this model has been optimized for observations of Eta Carinae (a bright source centered on CCD row 512 with the 52x0.1 and 52x0.2 slits). The properties of the scattered/diffuse background light may be dependant on the slit size and the location of the source relative to the CCD center. However, those relations are outside the scope of this report.

In this report we will refer to the low level of background spread out over the extent of the STIS CCD as "scattered light." We define scattered light as the signal that remains in the CCD pixels when the XSF (cross-dispersion profile) has been subtracted from a spectrum (for details on the XSF see Martin, 2004). Strictly speaking this might not be scattered light in the classical sense. As a result of the way we go about modeling the scattered light here we largely remove the STIS CCD spectroscopic ghost (Gull et. al, 2002; Hill, 2000) as part of the scattered light component. We are unable to determine where in the optical path these photons are from. However, for the purpose of this work we treat this background as scattered light.

In most situations, the scattered light contributes less than 10% of the total flux in a 1D spectrum extraction. However, in cases like Eta Carinae where we wish to observe features from a faint nebula in proximity to a bright source, this contribution is significant. The scattered light contribution can also be important when considering the

flux calibration of the STIS CCD. At the longest wavelengths covered by the STIS, the scattered light can account for a very significant fraction of the flux from the central source because it is spread over the entire CCD almost like a uniform background.

Gull, et al. (2002) reviewed the gross characteristics of scattered light on the STIS CCD in spectroscopic mode. The best way to visualize the scattered light contribution is to plot it as a function of CCD row number on the cross-dispersion axis. The scattered light distribution measured on the cross-dispersion axis peaks at one percent or less of the peak value of a bright source and falls off exponentially away from the source. The shape of this distribution changes as a function of wavelength (Figure 1). At shorter wavelengths the scattered light is more centrally concentrated and at longer wavelengths it becomes almost a constant contribution over the breadth of the CCD.

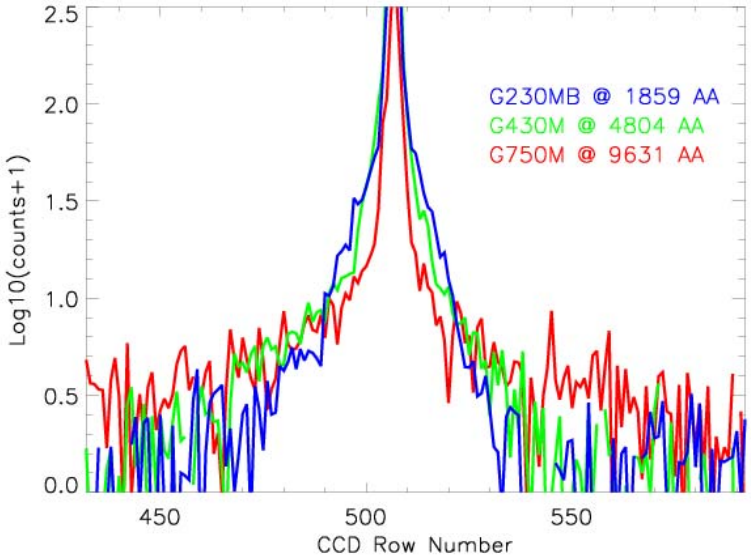

Figure 1 **The scattered light distributions plotted at three different wavelengths. The peak XSF value in each of these profiles is on the order of 10,000 counts.**

Figure 2 demonstrates that the scattered light is dependent on the positioning of the bright source on the slit. Note that when the source is placed on the top of the slit (near CCD row 900) the scattered light is not symmetric and has a significant "lump" centered about -60 rows from the peak. All the observations of Eta Carinae for the Treasury Project were taken with the star centered on the slit, so we focused on parameterizing the scattered light for that configuration. However this demonstrates that our findings in this report are probably not applicable to observations with the STIS CCD where the target is on the "alternate" aperture, significantly displaced from the center of the slit.

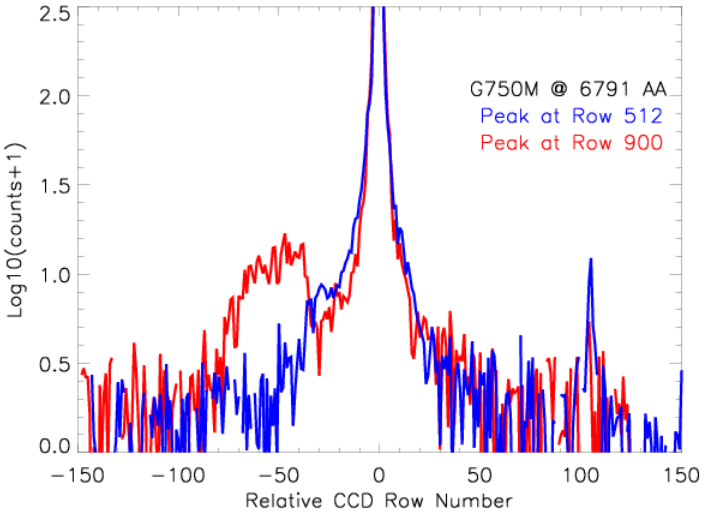

Figure 2 A comparison of the scattered light from a point source centered at row 512 versus row 900. On the STIS CCD one row is about 0.05". Note that the pixel scale for reduced data for the Eta Carinae Treasury Project is about 0.025"/pixel.

2. The Model

A number of different types of functions were investigated for modeling the scattered light distribution on the STIS CCD. We found that a squared Lorentzian fits the wings of the distribution much better than a Gaussian. This functional form was also used to model the cross-dispersion profile of a point source (the XSF) on the STIS CCD (Martin, 2004). The values of p and z are the same as presented in that model. Therefore, the model for the flux of scattered light as a function of CCD row number (x) is as follows:

$$f[x] = p * \left[c \left(\frac{a_n^{\,4}}{(a_n^{\,2} + (x - (z - b))^2)^2} \right) + d \right]$$

Where:

p = maximum peak value of XSF
z = the row number where the maximum peak value for the XSF resides
a_1 = the width of the scattered light profile when x > (z-b)
a_2 = the width of the scattered light profile when x < (z-b)
b = the offset of the center of the scattered light distribution measured with respect to the center of the XSF (z)
c = the ratio between the maximum of the scattered light distribution and the peak value of the XSF.
d = constant background level (hopefully works out to zero)

The scattered light distribution does not appear to be perfectly symmetric. It is skewed slightly to the side where x > (z-b) (direction of increasing row number on the CCD). To compensate for this effect, different peak width parameters (a_1 and a_2) are used to express

the shape of the function when x > (z-b) or x < (z-b). Note that when x = (z-b), at the center of the distribution that the f(x) is the same value whether a_1 or a_2 is used.

The variables p and z are determined by fitting the XSF, which will not be discussed here. For a full explanation of the XSF (cross-dispersed point spread function) and the variables p and z see Martin (2004). The constant background level (d) should be zero if the XSF and the scattered light contribution together account for all the observed flux while the remaining variables (a_1, a_2, b, and c) can be fit as functions of wavelength and CCD column.

This model describes the actual flux distribution while each pixel value is the flux integrated over the pixel's surface area. Therefore, to fit the observed scattered light distribution, we must integrate f[x]. This is represented by the function F[x]:

$$F[x] = \int f[x]dx$$

$$F[x] = \frac{pc}{2}\left[2d*(x-(z-b)) + \frac{a_n{}^2(x-(z-b))}{a_n{}^2 + (x-(z-b))^2} - a \times ArcTan\left[\frac{x-(z-b)}{a_n}\right]\right]$$

Given F[x], we assume that each pixel has a uniform sensitivity across its surface and that no significant gaps exist between pixels to arrive at:

$$Pixel\_Value(x) = F[x+0.5] - F[x-0.5]$$

3. Results

STIS CCD observations of single stars (point sources) were obtained from the MAST archive. The observations used to fit parameters to the scattered light were long exposures (with significant signal in the scattered component) which had the target centered on the slit (appearing near CCD row 512). The data were bias subtracted and flat fielded but not "rectified" and interpolated since any scheme which transforms the pixels has the effect of blurring the data.

Cross-sections of data including all CCD rows were extracted from the images by taking the median pixel value for each row from twenty consecutive CCD columns. The cross sections were made starting in column 10 and generating cross-sections at intervals of 10 columns to column number 1010. The columns on the edge of the CCD were excluded because they tend to be anomalous. The XSF of the point source was fit to the central part of each cross-section using the model described in Martin (2004) and subtracted from the cross-section. The constant term in the original XSF model is omitted here because it was initially included as a pseudo-scattered light correction.

The extracted cross-sections with the XSF subtracted were fit to the scattered light model (see previous section) using a modified Levenberg-Marquart method which was

developed and rigorously tested in-house. After rejecting fits which did not converge or had large chi-squares, there are 5643 fits covering a range of gratings, wavelengths, and CCD column numbers.

As expected, the d parameter is consistent with zero for all the fits. All of the other parameters have significant trends with respect to wavelength. Only the relative amplitude of the scattered light (c) has a significant trend with respect to CCD column number (y in raw pixels). The best-fit relations for these parameters as a function of wavelength (λ in angstroms) are:

Scattered light peak width (a1 and a2, Figure 3):

$$a_1 = (75.5) - (5.22\times10^{-2})\lambda + (1.89\times10^{-5})\lambda^2 - (2.69\times10^{-9})\lambda^3 + (1.37\times10^{-13})\lambda^4$$

$$a_2 = (46.2) - (3.83\times10^{-2})\lambda + (1.69\times10^{-5})\lambda^2 - (2.69\times10^{-9})\lambda^3 + (1.46\times10^{-13})\lambda^4$$

Scattered light peak offset from XSF peak center (b, Figure 4):

$$b = (-63.9) + (5.31\times10^{-2})\lambda - (1.53\times10^{-5})\lambda^2 + (1.67\times10^{-9})\lambda^3 - (6.15\times10^{-14})\lambda^4$$

Scattered light peak amplitude (as a fraction of XSF peak amplitude, Figure 4):

$$c = (2.436\times10^{-2}) - (7.418\times10^{-6})\lambda + (6.139\times10^{-10})\lambda^2 - (6.000\times10^{-7})y$$

The scattered light model with these parameters fits the low-level background present in STIS CCD data reduced by the Treasury Project data pipeline. Figure 5 shows that there is excellent agreement between cross cuts of the spectra of BD +75 325 (a stellar point source) and the scattered light model.

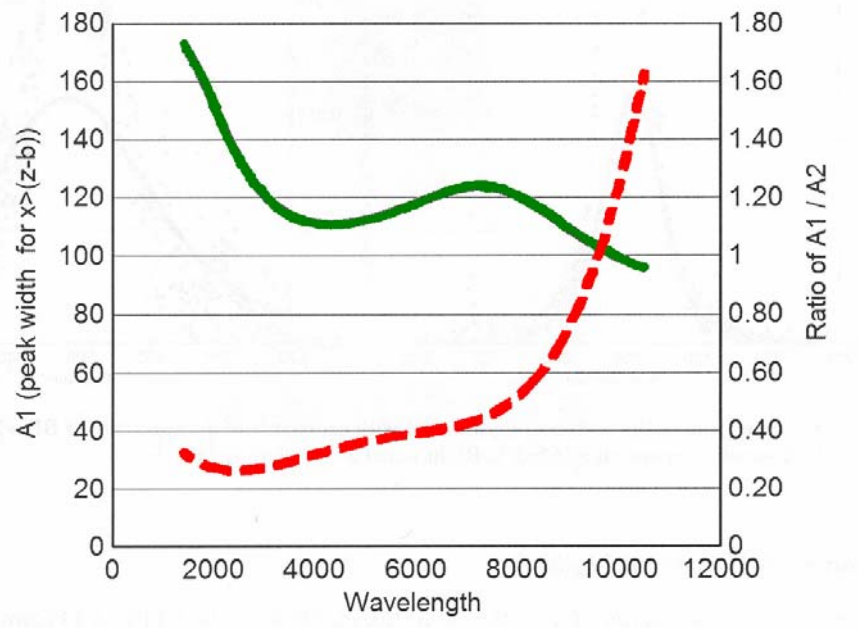

Figure 3 Parameter a_1 in red dotted line read off left axis and the ratio of a_1/a_2 in solid green read off left axis.

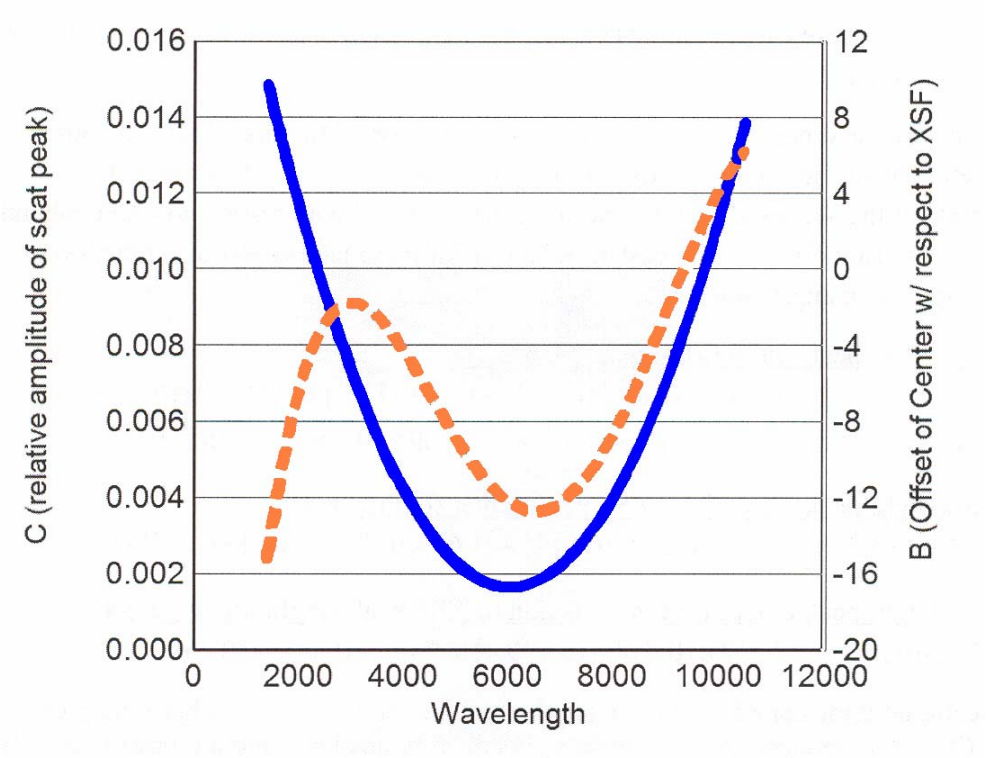

Figure 4 Best fit function for parameter c as the solid blue line read off the left axis and the best fit function for the b parameter as the dashed orange line read off the right axis.

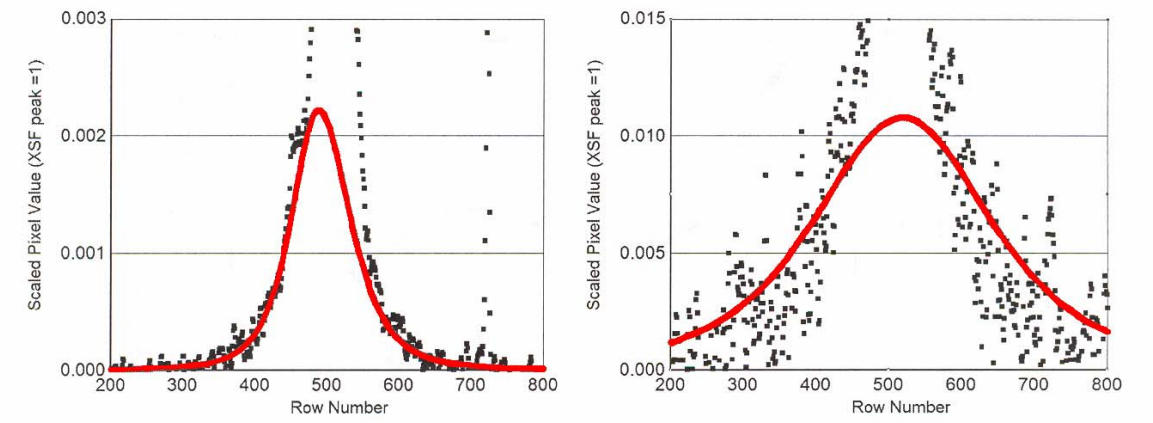

Figure 5 A comparison of the scattered light model with cross-cuts of the spectrum of BD +75 325. Left panel: a cross-cut at 6768 Å. Right panel: a cross-cut at 9851 Å.

4. Dealing with Scattered Light

The contribution of scattered light to the total flux incident on the STIS CCD from a point source is not trivial and must be accounted for in order to flux calibrate the spectrum within 5%. Figure 6 shows that the contribution from scattered light as a fraction of the total incident light on the STIS CCD from a point source varies roughly between 15% and 5% for wavelengths less than 9000 Å and contributes up to roughly

one half of the total flux at longer wavelengths. This shows one reason why it has traditionally been so difficult to obtain an accurate flux calibration for the STIS CCD at red wavelengths.

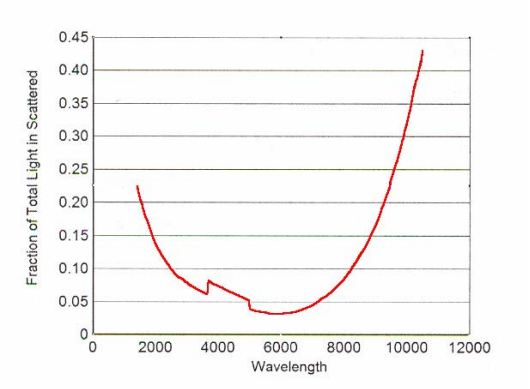

Figure 3 The fraction of flux in the scattered light component with respect to the total flux incident on the STIS CCD from a point source.

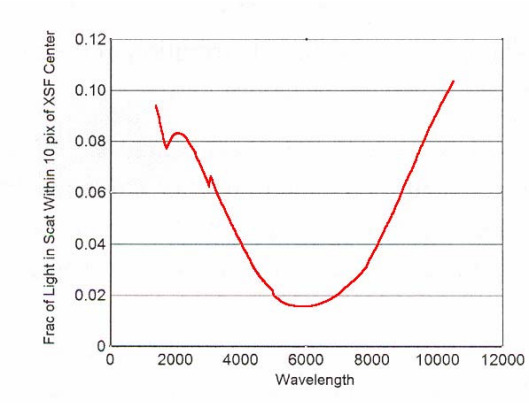

Figure 4 The fraction of flux within ten pixels of the XSF peak that is from the scattered light component.

When only the rows within 10 raw pixels of XSF peak are considered then the fraction of the flux contributed by scattered light is normally less than 10% of the total measured flux (Figure 7).

CALSTIS treats the scattered light contribution in a very simple-minded fashion. In point source spectral extraction mode, CALSTIS considers the scattered light a constant background which is measured at some remote distance from the peak of the XSF on the cross-dispersion axis and then subtracted from the ID extracted spectrum. In many cases the "background" measured in this way may not be representative of the scattered light contribution within a few rows of the XSF. This is particularly true at short wavelengths where the scattered component is more centrally concentrated and falls off significantly with increasing distance from the center of the XSF.

4.1 Theoretical Application

Our model for the scattered light distribution makes it possible to subtract the scattered light contribution in a more sophisticated manner. For a point source 1D extraction within a few original CCD rows of the XSF center, the scattered light background is reasonably approximated as a constant contribution which can be calculated from the peak value of the XSF and parameter c from the scattered light model (fractional amplitude of the scattered light, see Figure 5).

An extended source is a more complex case where the scattered light contribution must be convoluted with the flux distribution of the source in order to accurately quantify the amount of scattered light in each pixel. Therefore, the scattered light from an extended source as a function of row number (S(x)) becomes:

$$S(x) = \int_{-\infty}^{\infty} \varphi(u) \left[cp \frac{a_n{}^4}{(a_n{}^2 + (x - u - (z - b))^2} \right] du$$

Where φ(u) is the flux distribution of the extended source and a, b, c, p, and z are the same parameters as before.

As an example, we have calculated the scattered light for a bright point source surrounded by a fainter nebula. This φ(u) can be approximated as a function of constant value within so many pixels of the point source plus a delta function of appropriate amplitude at the location of the point source. In this case, S(x) becomes:

$$S(x) = cp \left\{ \left[\frac{a_n{}^4}{(a_n{}^2 + (x - (z - b))^2} \right] + \varphi_0 \left[\frac{a_n \left(2a_n r(a_n{}^2 - \delta\beta) - (a_n{}^2 + \delta^2)(a_n{}^2 + \beta^2) \right) \left(ArcTan\left(\frac{\delta}{a_n} \right) - ArcTan\left(\frac{\beta}{a_n} \right) \right)}{2(a_n + \delta^2)(a_n{}^2 + \beta^2)} \right] \right\}$$

$$\delta = (b - r + x)$$

$$\beta = (b + r + x)$$

φ_0 is the constant flux value of the surrounding nebula given as a fraction of the XSF peak value for the central source and r is the radius of the nebula on the cross dispersion axis given in original pixels. When r or φ_0 are small, the function reverts to the form given for a point source. Therefore, the nebula must be more than a few percent the brightness of the point source or have a large spatial extent in order to contribute significantly to the scattered light. Because of this, at most wavelengths we can model the scattered light for our Eta Carinae observations as the contribution from the central star alone since the contribution from the surrounding Homunculus nebula is negligible.

4.2 Practical Application

Figure 8 demonstrates the practical application of this model to remove the scattered light from the spectrum of a point source. Removal of the scattered light makes it easier to identify faint features in close proximity to the point source, such as the "railroad track" ghost image (Gull et al., 2002) below the main XSF peak.

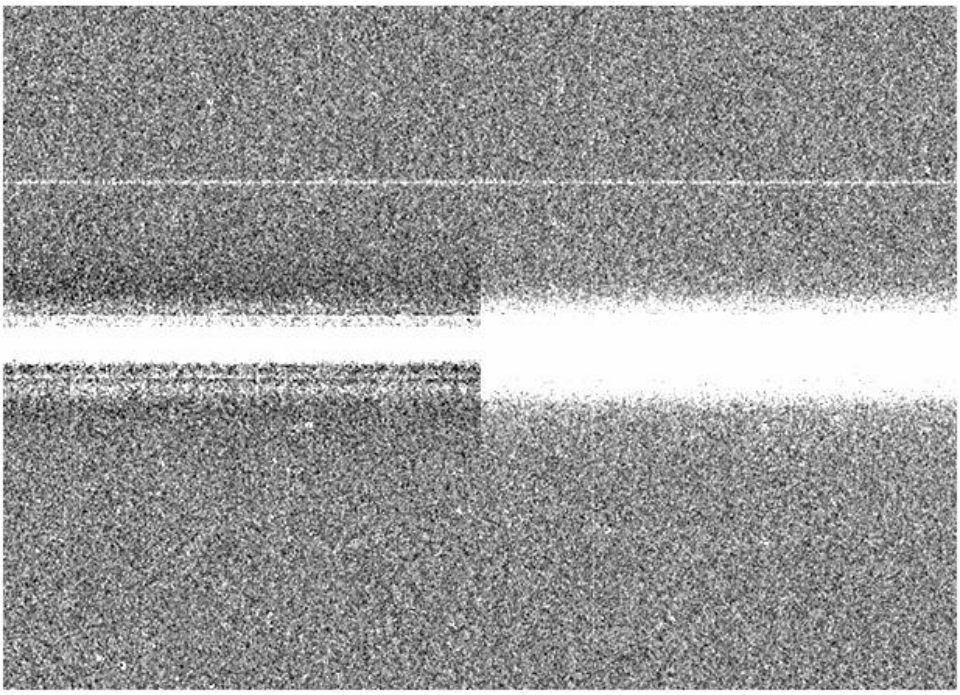

Figure 8 The spectrum of a point source before (right) and after (left) removal of the scattered light. The pixel brightness is on a linear scale with the contrast set by the standard "zscale" method.

A simple minded application of this model would vary the peak intensity of the scattered light (p) with wavelength in exact phase with the spectrum. However, in reality light is scattered both perpendicular and parallel to the dispersion axis.

Ideally, we could solve this problem by modeling the scattered light distribution in a spectrum from a point source with a very bright and very narrow emission feature. However, we could find no suitable spectrum of this type in the STScI archive. The strong Balmer absorption lines of an A type star should have the same effect as a strong emission line, only in reverse. So alternatively, we looked at the very high signal data gathered for Vega by Bohlin & Gilliland (2004). Examination of this data showed that there was no trace of the strong Balmer absorption lines in the scattered/diffuse light component. It turned out that the scattered/diffuse light was actually best fit by setting the peak value (p) in each column equal to the flux of the smoothed continuum without the Balmer lines.

This result is vaguely puzzling since it is only logical that the light from a point source should scatter in two dimensions and not just along the cross-dispersion axis. However, it is possible that the scattered light is so smoothed and muddled that taking the smoothed continuum value in the column is actually a very good approximation of the multiple degenerate components which actually contribute light in any given CCD column. At least this is the only explanation we have for a solution that clearly works in practice.

Without the detailed knowledge of the optical layout of the STIS we are unable to verify from first principles that this explanation is correct.

The Eta Carinae HST Treasury Project will make the software which removes the scattered light from STIS CCD images using these methods available on our website. It should be noted that these methods are applicable to other HST STIS observations made with the 52x0.2 or 52x0.0l slit on the main aperture and are very helpful for extracting the spectrum of any object in close proximity to a bright point source.

References:

Bohlin, R. C. & Gilliland, R. L. 2004, AJ, 127, 3508

Gull, T., Lindler, D., Tennant, D., Bowers, C., Grady, C., Hill, R.S., and Malumuth, E., 2002, "The STIS CCD Spectroscopic Line Spread Functions" presented at the 2002 HST Calibrations Workshop. (S Arribas, A Koekemoer, and B. Witmore, eds.)

Hill, R. S. 2000, "The Geometry and Approximate Correction of STIS CCD Window Ghosts," STIS Post-Launch SMOV Report #063, (Goddard Space Flight Center: Greenbelt)

Martin, J. C. 2004, "The STIS CCD Cross-Dispersion Point Spread Function," Eta Carinae Treasury Project Technical Report #2, http://etacar.umn.edu/treasury/publications/pdf/tmemo002.pdf